Sensitivity of the Amundsen Sea Low to Stratospheric Ozone Depletion

RYAN L. FOGT AND ELIZABETH A. ZBACNIK

Scalia Laboratory for Atmospheric Analysis and Department of Geography, Ohio University, Athens, Ohio

(Manuscript received 24 October 2013, in final form 10 September 2014)

ABSTRACT

Dramatic sea ice loss in the Amundsen and Bellingshausen Seas and regional warming in West Antarctica and the Antarctica Peninsula have been observed over the last few decades. Both of these changes are strongly influenced by the presence of the Amundsen Sea low (ASL), a climatological region of low pressure in the Amundsen Sea. Studies have demonstrated a deepening of the ASL, particularly in austral spring and to a lesser extent autumn, the former related to decreases in the underlying cyclone central pressures and the latter previously suggested to be due to stratospheric ozone depletion.

This study further investigates the sensitivity of the ASL to stratospheric ozone depletion using geopotential height from a suite of chemistry–climate models (CCMs) as well as historical simulations from phase 5 of the Coupled Model Intercomparison Project (CMIP5). Overall, both model types capture the mean characteristics of the ASL, although they have notable positive height biases at 850 hPa and a subdued seasonal cycle in its longitudinal position. Comparing across model simulations, it is observed that there is a pronounced influence of stratospheric ozone depletion in the vicinity of the ASL in the stratosphere through the lower troposphere during austral summer, consistent with the positive phase of the southern annular mode. In the autumn, the authors note a weaker, secondary influence of stratospheric ozone depletion on the ASL only in the CMIP5 simulations.

1. Introduction

The Southern Hemisphere atmospheric circulation in the troposphere and stratosphere has been influenced by stratospheric ozone depletion over the last several decades. Perhaps the most notable impact in the stratosphere is the presence of the ozone hole during spring and the resultant stratospheric cooling which extends into early summer (Randel and Wu 1999; Thompson and Solomon 2002; Kindem and Christiansen 2001; Son et al. 2010; WMO 2011). Other stratospheric circulation impacts include the strengthening of the polar night jet (Arblaster and Meehl 2006; Akiyoshi et al. 2009) and the delayed break-up of the polar vortex (e.g., Akiyoshi et al. 2009; WMO 2011). In the troposphere, previous work has noted that the positive trend in the southern annular mode (SAM) index during summer over the past 50 years or so (Marshall 2003, 2007; Thompson and Solomon 2002) is associated primarily with stratospheric ozone depletion through both observational (Thompson and Solomon 2002) and modeling studies (Arblaster and Meehl 2006; Perlwitz et al. 2008; Fogt et al. 2009a), resulting from an increased pressure gradient between the mid and high latitudes and stronger circumpolar westerly winds. More recently, a study by Son et al. (2010) has shown that the Southern Hemisphere westerly jet has not only intensified, but also is displaced more poleward, in conjunction with a poleward expansion of the Hadley cell.

As noted by these examples, much of the previous work on the impacts of stratospheric ozone depletion across the Southern Hemisphere has focused on large-scale climate features, rather than a particular geographic location or smaller-scale feature of the atmospheric circulation. In a more regional study, Turner et al. (2009) examined how changes in sea ice extent are connected with changes in atmospheric circulation and, using an atmosphere-only climate model (the atmospheric component of version 3 of the Hadley Center climate model, HadAM3), investigated whether these changes can be attributed to stratospheric ozone depletion. Examining the 500-hPa geopotential heights for 1979–2006, they noted a deepening in austral autumn of the Amundsen Sea low [ASL; previously called the "Amundsen-Bellingshausen Seas Low" by Fogt et al. (2012) and Hosking et al. (2013)], a climatological region

Corresponding author address: Ryan L. Fogt, Department of Geography, Ohio University, 122 Clippinger Laboratories, Athens, OH 45701.
E-mail: fogtr@ohio.edu

DOI: 10.1175/JCLI-D-13-00657.1

of low pressure off the coast of West Antarctica, which they attribute to stratospheric ozone depletion. A deeper ASL, through implied geostrophic wind changes and thermal advection, produces an increase in sea ice extent in the Ross Sea but a decrease in the Amundsen and Bellingshausen Seas, consistent with observations (Zwally et al. 2002; Holland and Kwok 2012). This decrease of sea ice in the Amundsen and Bellingshausen Seas region is statistically significant only in austral autumn [March–May (MAM)]. However, the influence of ozone on the Antarctic climate in MAM is somewhat inconsistent with the observational study by Thompson and Solomon (2002), who found the largest near-surface atmospheric circulation ozone-related changes over Antarctica during December and January (i.e., summer), with only a possible secondary impact in autumn (i.e., trends exceeding one standard deviation near the surface from December to May).

Regardless of the mechanism driving the ASL changes, other studies have linked the ASL to sea ice and other Antarctic regional climate variations, highlighting its importance. Because of its location in the vicinity of the Amundsen and Bellingshausen Seas (approximately 55°–75°S, 180°–90°W), the presence of the ASL leads to sustained north-northwesterly flow along the eastern side of the low and south-southeasterly flow along the western side, thereby advecting warm/moist air near the Antarctic Peninsula and Bellingshausen Seas and cold/dry air off West Antarctica over the Ross Sea. Winds associated with atmospheric circulation anomalies in the ASL region have been shown to lead to convergence of sea ice in the Bellingshausen/eastern Amundsen Seas (Massom et al. 2008), in addition to a decrease in sea ice season length (Stammerjohn et al. 2008); opposite conditions have been observed in the western Amundsen and Ross Seas. A study by Holland and Kwok (2012) indicates that wind-driven changes in ice advection associated with the ASL near West Antarctica explain the majority of sea ice concentration trends there.

The impact of the ASL circulation is also seen in surface temperature trends since the International Geophysical Year (IGY), which indicate spring and winter warming over the Antarctic Peninsula and West Antarctica (Steig et al. 2009; O'Donnell et al. 2011) that has been tied to tropical sea surface temperature variations (Schneider et al. 2012; Ding et al. 2011). In contrast, summer warming along the eastern Antarctic Peninsula is more strongly tied to changes in the SAM (Marshall et al. 2006; Orr et al. 2008). Fogt et al. (2012) studied the variability of the ASL in terms of its interannual position and magnitude. They found that the position of the ASL is strongly tied to the location of the maximum cyclone system density while its magnitude is related to both cyclone system density and central pressure. In their climatology of the ASL, Turner et al. (2013) note connections between the ASL and large-scale modes of climate variability, including the El Niño–Southern Oscillation phase (located farther west and deeper during a La Niña, and vice versa for El Niño, although only the changes in strength are significant), the SAM (farther south and deeper during positive SAM phases), and the zonal wave-3 pattern (Raphael 2004) common in this region. Similarly, Hosking et al. (2013) find many connections between the location and intensity of the ASL and many climate parameters (temperature, wind, precipitation) across the Antarctic Peninsula and West Antarctica.

Given its influence on the local climate, it is important to further understand how the ASL has responded historically to external forcing, such as changes in greenhouse gas concentrations or stratospheric ozone depletion. While the Turner et al. (2009) study has shed some light on these processes, the model they employed was an atmosphere-only model with prescribed levels of ozone, thereby not allowing the ozone hole to develop on its own and not allowing for other interactions such as between the ocean and atmospheric chemistry. It is also necessary to understand if similar changes in the ASL are seen in other model simulations, especially given that they note the largest changes in austral autumn when the impact of stratospheric ozone depletion on the Southern Hemisphere climate is less well understood.

Multiple studies have shown the advantages of using chemistry–climate models (CCMs) to study the effects of stratospheric ozone depletion on atmospheric circulation (e.g., Eyring et al. 2007; Perlwitz et al. 2008; Fogt et al. 2009b; Son et al. 2010). These models are relatively new and include fully interactive stratospheric ozone chemistry, thereby allowing for a two-way interaction between ozone and the atmosphere. They are also able to account for atmospheric dynamics better and often have a higher vertical resolution in the stratosphere than other models, therefore making them valuable tools in understanding climate change and stratospheric ozone depletion connections; however, they are atmosphere-only models with no coupling to an ocean. To investigate the possible role of ocean coupling, a suite of historical simulations from phase 5 of the Coupled Model Intercomparison Project (CMIP5) are employed. This paper examines the sensitivity of the ASL to stratospheric ozone depletion using these models in order to expand upon and test the sensitivity of the results presented by Turner et al. (2009). Section 2 provides information on the CCMs, CMIP5 simulations, reanalysis, and ozone observational data used. This is followed in section 3 by an examination of the climatological seasonal cycles in geopotential height, MSLP, and total column ozone in order to evaluate the

TABLE 1. CCMVal-2 models used in this study. Included information is the full model name, the resolution before interpolation, the number of vertical levels in the original model, and the number of simulations in the REF-B1, REF-B2 and SCN-B2b runs.

Model name	Full name	Initial resolution (degrees)	No. of levels	REF-B1/B2	SCN-B2b
CCSRNIES	Center for Climate System Research/National Institute for Environmental Studies	2.8125 × 2.8125	34	3/1	1
CMAM	Canadian Middle Atmosphere Model	5.625 × 5.36	71	3/3	3
MRI	Meteorological Research Institute	2.8125 × 2.8125	68	3/2	1
SOCOL	Solar-Climate-Ozone Links	3.75 × 4	39	3/3	1
UMETRAC	Unified Model with Eulerian Transport and Atmospheric Chemistry	3.75 × 2.5	64	1/0	
UMSLIMCAT	Unified Model – UMSLIMCAT	3.75 × 2.5	64	1/1	1

overall performance of the model simulations in the high southern latitudes. Section 4 describes the sensitivity of the ASL to stratospheric ozone depletion based on geopotential height changes in the models. A discussion and concluding remarks are offered in section 5. All seasons refer to the Southern Hemisphere.

2. Data and methods, and models and simulations

a. *Chemistry–climate models*

The seasonal CCM simulations are from models participating in the second phase of the Chemistry–Climate Model Validation project (CCMVal-2), a model intercomparison project used within the World Meteorological Organization's (WMO's) 2010 ozone assessment report. (SPARC CCMVal 2010). Pertinent details on the simulations used in this study, including expansions of model names, are described below and in Table 1; more detailed descriptions of the models and their configurations and biases can be found in Morgenstern et al. (2010) and SPARC CCMVal (2010).

For CCMVal-2, various modeling centers provided multiple simulations, including a historical simulation encompassing the years between 1960 and 2006, a forecast simulation covering the period between 1960 and 2100, and various scenario simulations (e.g., greenhouse gas concentrations fixed at specified levels, no ozone depletion, etc.) also covering 1960–2100 (Eyring et al. 2008). This study focuses on three of the simulations: the two reference runs (REF-B1 and REF-B2) and one of the sensitivity scenarios (SCN-B2b). REF-B1 is the simulation of past conditions and therefore includes both anthropogenic and natural forcings taken from observations (Eyring et al. 2008; Morgenstern et al. 2010; SPARC CCMVal 2010). REF-B2, being a forecast simulation and extending to year 2100, emphasizes the effects of anthropogenic forcings and therefore natural forcings are excluded (Eyring et al. 2008; Morgenstern et al. 2010; SPARC CCMVal 2010). In the REF-B2 experiments greenhouse gas concentrations are taken from the Intergovernmental Panel on Climate Change (IPCC) Special Report on Emission Scenario (SRES) A1B simulation, while ozone-depleting substances are based on an adjusted version of the WMO A1 scenario (Morgenstern et al. 2010). We also investigate changes in the circulation in the sensitivity scenario SCN-B2b, which has fixed concentrations of the ozone depleting halogens (at their concentrations in year 1960), and therefore does not produce an ozone hole. Using the SCN-B2b scenario therefore allows for an investigation of the role of stratospheric ozone depletion on the climate when comparing it directly to REF-B2 (Eyring et al. 2008).

Data from 18 models were submitted to the CCMVal-2 project; however, not all models provided members for each of the simulations and not all models provided the geopotential height and total column ozone variables that are investigated in this study; furthermore, the CCMs were only considered if data were available for each of the REF-B1, REF-B2, and SCN-B2b simulations. Table 1 lists the subset of models used here as well as the number of ensemble members for each simulation. For the CCMs, only a subset of the available years (1979–2004) is examined, as this is the period when the most of this type of model data are available. For models with more than one ensemble member within a particular simulation, a model mean is computed before it is included in the grand-ensemble mean, thereby giving equal weight to each model rather than each ensemble member.

b. *CMIP5 simulations*

Only one model (CMAM) has an interactive ocean in the REF-B2 simulations; the sea surface temperatures/sea ice concentrations are prescribed from coupled global climate model simulations in the other four CCMs. To better understand the role of coupling to an ocean, which may be important in the lower troposphere where the ASL is most marked, a suite of historical simulations from the CMIP5 archive (Taylor et al. 2012) is employed (Table 2; expansions of relevant CMIP5 model names are given there). We make use of two separate groups,

TABLE 2. CMIP5 models used in this study. Included information is the full model name, the approximate horizontal resolution before interpolation, the number of vertical levels, and the number of ensemble members with geopotential height data. All CMIP5 simulations except for CSIRO were for the ozone-only historical experiment, where only ozone concentrations were prescribed.

Model name	Full name	Initial resolution (degrees)	No. of levels	No. of ensemble members
CCSM4	Community Climate System Model, version 4	1.25 × 0.9375	17	3
FGOALS	Institute of Atmospheric Physics Flexible Global Ocean–Atmosphere–Land System Model gridpoint, version 2	2.8125 × 3.0	17	1
GISS_EH	Goddard Institute for Space Studies Model E, coupled with the Hybrid Coordinate Ocean Model	2.5 × 2.0	17	5
GISS_ER	Goddard Institute for Space Studies Model E, coupled with the Russell ocean model	2.5 × 2.0	17	5
CSIRO*	Commonwealth Scientific and Industrial Research Organization Mark 3.6.0	1.875 × 1.845	18	10 (historical) 5 (no-ozone)

* This model included both the historical simulation with all forcing agents and a no-ozone simulation, where all other forcing agents except ozone were prescribed during the twentieth century.

a simulation of the twentieth century consisting of four separate models where only ozone is prescribed and other forcing agents are set to a fixed climatological cycle (hereinafter denoted as CMIP5), and two historical simulations from the Commonwealth Scientific and Industrial Research Organization (CSIRO) model, one with all the forcing agents prescribed throughout the twentieth century, and another where there are no ozone changes in the twentieth century (with the "no-ozone" simulation hereinafter denoted as CSIRO), but all other forcing agents evolve. Comparing the multimodel means from these two simulations will both help to understand the role of stratospheric ozone depletion (since ozone is the only forcing agent altered in the simulations) as well as the role of coupling to an ocean. Another notable difference in these simulations from the CCMs is that they include tropospheric ozone increases, which may also impact the atmospheric circulation; investigating these processes however is beyond the scope of the paper (which focuses on stratospheric ozone depletion). While more models from other experiments would have been beneficial, these were the most relevant historical simulations to our study with archived geopotential height data. Further, each CMIP5 model has multiple ensemble members, thereby increasing the likelihood of identifying the forced response from stratospheric ozone depletion. The CMIP5 data are also analyzed during the 1979–2004 period.

c. *Atmospheric reanalyses*

In addition to the model data described above, monthly mean geopotential height and mean sea level pressure (MSLP) fields from three reanalyses are also used, namely the National Centers for Environmental Prediction (NCEP) Climate Forecast System Reanalysis (CFSR; Saha et al. 2010), the Interim European Centre for Medium-Range Weather Forecasts (ECMWF) Re-Analysis (ERA-Interim; Dee et al. 2011), and the Japan Meteorological Agency and Central Research Institute of Electric Power Industry 25-yr reanalysis (Onogi et al. 2005). A multireanalysis mean is routinely employed to investigate the mean conditions observed across each reanalysis.

All model and reanalysis data were investigated using a 2.5° × 2.5° latitude/longitude resolution; this is much coarser than the reanalyses but is the middle range for most CCMs and CMIP5 simulations. While at times the individual CCMs and reanalyses are considered, we primarily focus on the multimodel and individual model means of the CCM, CMIP5, and CSIRO simulations (to better highlight the forced response) and a separate mean for all three reanalyses.

d. *Ozone observations*

To determine how well the CCMs capture the ozone hole, an updated version of the Bodeker et al. (2001) gridded total column ozone dataset is employed (Bodeker et al. 2005). This dataset uses a blend of multiple satellite-derived ozone data, validated and adjusted independently using ground-based Dobson spectrophotometer data.

3. Model validation

a. *Climatological seasonal cycle of 850-hPa geopotential heights and MSLP*

The ASL is a feature of the lower troposphere that is broadly defined as the region of lowest MSLP in the vicinity of the Amundsen and Bellingshausen Seas (Fogt et al. 2012; Hosking et al. 2013; Turner et al. 2013). However, MSLP data are not available for any of the CCMVal-2 models. While surface pressure is available, it is too noisy in the region due to the various model resolutions and steep topographic gradients of the Antarctic Peninsula and coastal West Antarctica, and therefore does not depict the

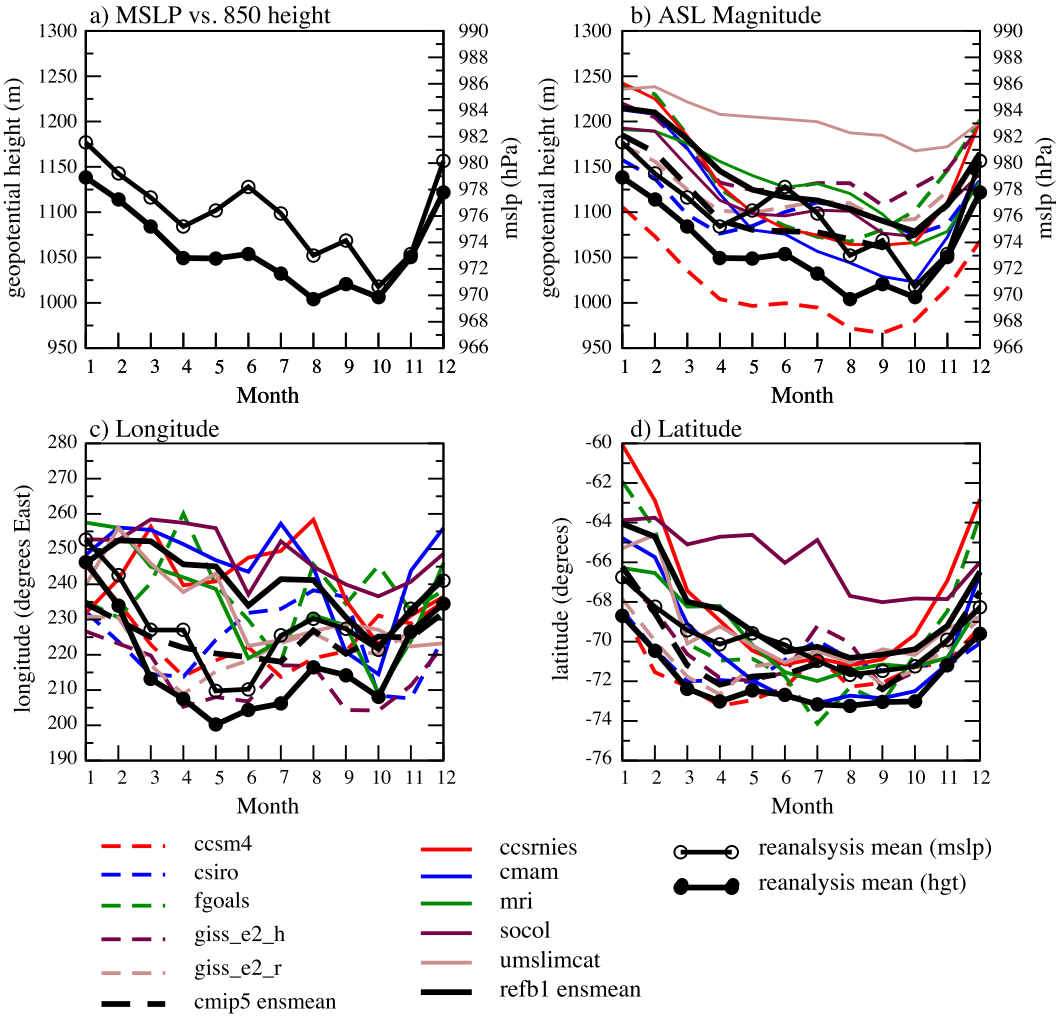

FIG. 1. Climatological (1979–2004) seasonal cycle in the ASL region (defined as 55°–75°S, 180°–60°W) of (a) the magnitude of the minimum in multireanalysis MSLP and 850-hPa geopotential heights (model and reanalysis mean 850 hPa), (b) ASL magnitude, (c) longitudinal position, and (d) latitudinal position.

ASL as straightforwardly. To examine if 850-hPa geopotential heights can be used instead as a proxy for near-surface conditions, the magnitude and location of the lowest monthly mean MSLP and 850-hPa height minimum values in the ASL region (defined hereinafter as 55°–75°S, 180°–60°W) averaged over 1979–2004 are compared in the multireanalysis mean (Fig. 1a). While dampened, the seasonal cycle of the 850-hPa height minima follows that of the MSLP, although the local maxima associated with the semiannual oscillation in June are absent. Hosking et al. (2013), who defined the ASL based on the relative minimum sea level pressure in the ASL region rather than the absolute minimum as done in Fig. 1a, do not observe this maximum in June. Thus, this feature is sensitive to the method used to define the ASL and therefore it is not surprising that it is not observed as strongly at 850 hPa. Given the other similarities, the 850-hPa geopotential heights provide a useful depiction of the ASL variability and will be used throughout this study.

Figures 1b–d show the mean magnitude, longitude, and latitude, respectively, for the 850-mb height minima in the ASL region from the various model simulations (CCMs are solid lines, CMIP5 dashed). It is evident that most of the models (with the exception of CCSM4) have heights that are too high and therefore too weak of an ASL (Fig. 1b). Nonetheless, the seasonal cycle of the ASL magnitude and the timing of the strongest ASL during October are typically well captured in most model simulations. Using reanalysis MSLP data, Fogt et al. (2012) found that the ASL has a pronounced east–west and north–south seasonal migration between the Ross Sea region and the Antarctic Peninsula, where it is farthest east during austral summer [December–February (DJF)] and farthest west during austral winter [June–August

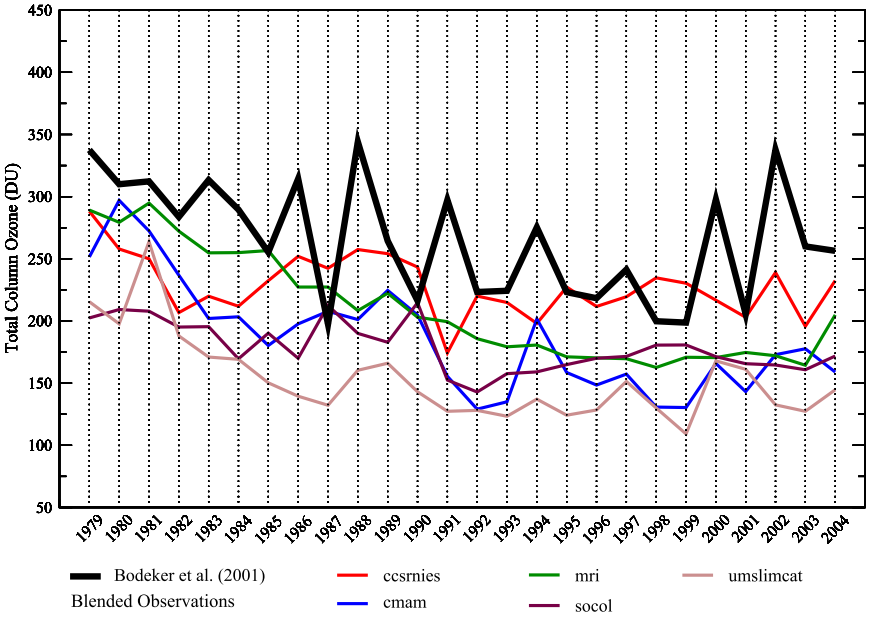

FIG. 2. Area-averaged (70°–90°S) monthly mean October total ozone column values for 1979–2004 for all of the REF-B1 models (colored lines) and the Bodeker et al. (2001, 2005) blended gridded ozone observations.

(JJA)]. Although reflected somewhat in the multimodel mean for both CCMs and CMIP5 (heavy lines in Fig. 1c), the longitudinal positioning of the ASL in individual models is quite variable and many have a less pronounced longitudinal seasonal progression of the 850-hPa height minimum. The problems in capturing the longitudinal position of the ASL were noted in nearly all CMIP5 simulations by Hosking et al. (2013), and likely reflect intermodel variations in the underlying synoptic activity or the phase and amplitude of the planetary waves in the Southern Hemisphere, both which influence the seasonal east–west movement of the ASL (Lachlan-Cope et al. 2001; Fogt et al. 2012; Turner et al. 2013). Despite the problems in the longitudinal position, the seasonal cycle of latitudinal position (Fig. 1d) is well simulated in all models, although they do tend to have an ASL that is farther north than in the reanalyses. Based on Figs. 1b–d, in general the seasonal cycle of the ASL is captured sufficiently well by the CCMs and the CMIP5 simulations, especially in the multimodel mean (thick black lines in Figs. 1b–d), which is primarily used in our analyses.

b. *Changes in total column ozone*

To assess the simulation of the ozone hole in the CCMs, monthly mean total column ozone values for the month of October are area-averaged over the polar cap (70°–90°S) and then compared to gridded blended ozone observations of Bodeker et al. (2001, 2005) in Fig. 2. Notably, both CCSRNIES and SOCOL have too small of a change in the total column ozone over the study period in these models; changes in the polar-cap averaged total column ozone in these models over the study period are approximately 35–50 Dobson units (DU), compared to 80–120 DU seen in the other models and observations. Additionally, the observations have notable spikes in 1988 and 2002, years marked with strong stratospheric warming episodes, a weaker vortex, and little ozone depletion over Antarctica (Hio and Yoden 2005; Roscoe et al. 2005). Given that the atmospheric chemistry is interactively simulated in the CCM simulations, it is not surprising that the models do not represent these individual spikes well as they were driven by changes in stratospheric dynamics; further, the model ensemble means are displayed in Fig. 2, which masks a considerable portion of the interannual variability. However, the recent higher values in 2000 and 2002 in observations reduce the magnitude of the observed stratospheric ozone depletion when compared to the models, as will be discussed in the following section.

4. Influence of stratospheric ozone depletion

a. *Area-averaged linear height changes*

To understand the influence of stratospheric ozone depletion on the atmospheric circulation, linear height changes are first examined in Fig. 3 using area averages over the polar cap and the ASL region, during 1979–2004 by month. The height changes are calculated using

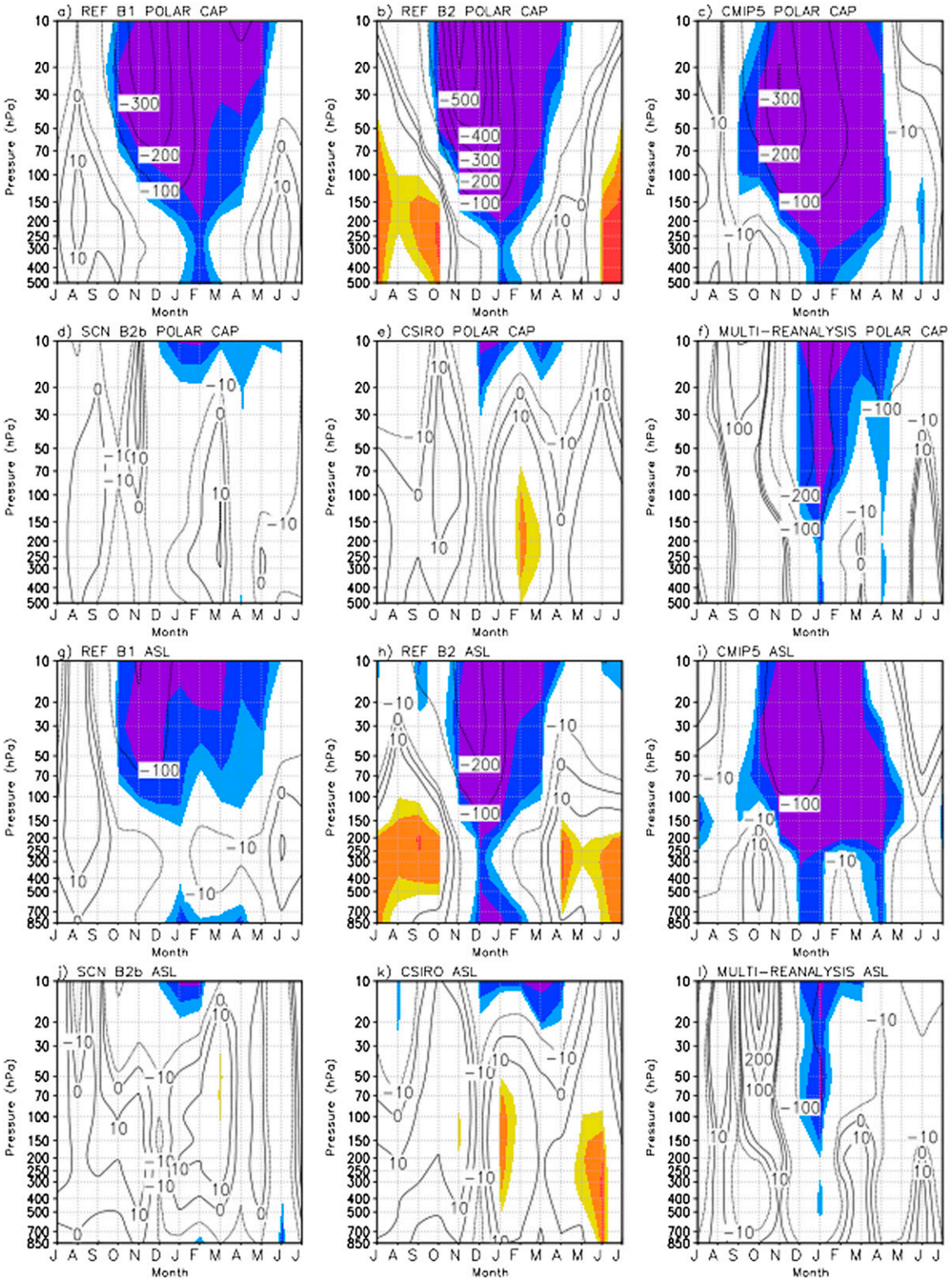

FIG. 3. Area-averaged linear height changes, 1979–2004, over the polar cap (70°–90°S; top two rows) and the ASL region (bottom two rows). Solid lines indicate height rises while dashed lines are height falls. Primary contour interval is 100 m, with an additional contour at ±10 m. Shading (from dark to light shades) indicates changes statistically different from zero in the multimodel mean at $p < 0.01$, $p < 0.05$, and $p < 0.10$.

the slope of the linear least squares regression line multiplied by 26 (the number of years encompassed in the 1979–2004 period); changes statistically different from zero in the multimodel means are shaded in Fig. 3 (from dark to light shading, $p < 0.01$, $p < 0.05$, $p < 0.10$). The effect of stratospheric ozone depletion on height falls over the polar cap is clearly evident in the second row of Fig. 3, as the SCN-B2b scenario (Fig. 3d) and CSIRO no-ozone simulation (Fig. 3e) only have significant height falls in the upper stratosphere, compared to the other simulations which show significant changes in the summer throughout the stratosphere and troposphere. Compared to the reanalyses, the CCMs and CMIP5 simulations (Figs. 3a–c) have the maximum height changes much higher in the stratosphere, and the magnitude is much greater in the models, especially in REF-B2 (Fig. 3b). The larger height changes in the CCMs are due to the reduced interannual variability and particularly the relatively higher concentrations in 2002 of polar-cap ozone as observed in Fig. 2; model trends calculated from 1979–2001 (not shown) are in much closer agreement with the reanalyses. Despite the larger values, the seasonal cycle of the height changes and their downward propagation in the models are consistent with the reanalysis mean, and with the timing in the observational study by Thompson and Solomon (2002). Over the ASL region (bottom two rows of Fig. 3), there is evidence of statistically significant stratospheric ozone depletion-induced height falls in the stratosphere in both the models (Figs. 3g–i) and the reanalyses (Fig. 3l), although the magnitude of these is much smaller than over the polar cap. Furthermore, the influence on the tropospheric circulation in the ASL region is much less clear in both the models and the reanalyses; over the polar cap, REF-B1, REF-B2, and the reanalysis means all clearly show height falls existing at least during austral summer, while there are more mixed results of the timing, duration, and amplitude of the lower troposphere height falls over the ASL region.

We identify a significant response to stratospheric ozone depletion based on approaches in previous studies (i.e., Gillett et al. 2013; Sigmond and Fyfe 2014). First, a statistically significant trend in the CMIP5 simulations (which only contain forcing from ozone changes) must be observed. For the others, there must be a statistically significant difference in the trends between the simulations with all forcings and those without stratospheric ozone depletion (i.e., between the REF-B2 and SCN-B2b for the CCMVal-2 simulations, or the CSIRO historical and CSIRO no-ozone simulations). To better understand the role of stratospheric ozone depletion on the height changes under these conditions, area averaged geopotential heights as in Fig. 3 are first considered.

The lower stratospheric geopotential height trends/differences (at 100 hPa) are examined seasonally over the polar cap and ASL region in Figs. 4 and 5, respectively. For both the trends and trend differences (red data in panels b and d), the error bars represent the 95% confidence intervals based on the multimodel (or multireanalysis or CSIRO ensemble) mean. Notably, the REF-B1 trends mirror the reanalysis trends in terms of the seasonal cycle and magnitude in both Figs. 4a and 5a. Over the polar cap and the ASL region, the trends are most negative in DJF and least negative/most positive in JJA in all model means studied. In agreement with Fig. 3, over the polar cap (Fig. 4), there are statistically significant trends in austral summer in all simulations with stratospheric ozone depletion, as well as significant differences in the trends between the REF-B2/SCN-B2b and two groups of CSIRO historical simulations. Combined with significant trends in the ozone-only CMIP5 simulations, these characteristics clearly highlight the role of stratospheric ozone depletion at 100 hPa over both the polar cap and the ASL region in austral summer. Notably, the CMIP5 model mean trends are also statistically significant in MAM and SON over both the polar cap and ASL region (Figs. 4c and 5c). However, there are no significant differences between the REF-B2/SCN-B2b simulations outside of austral summer in either region (Figs. 4b and 5b), and only over the ASL region are there differences in these seasons between the two historical CSIRO simulations (Figs. 4d and 5d). It is possible that a weaker ozone-related signal exists in the seasons surrounding austral summer (reflected also in Fig. 3), but because of model differences in the significance of these trends, a clear ozone-related signal is only detectable in austral summer.

The changes in the ASL are more specifically investigated in Fig. 6, which depicts the height trends at 850-hPa area-averaged over the ASL region. Because of the high interannual variability in the region (Connolley 1997; Fogt et al. 2012; Turner et al. 2013), the range for the confidence intervals for the reanalyses and most model simulations includes zero in all seasons. Turning first to the reanalyses, Fogt et al. (2012) demonstrated that both the Japanese 25-yr and the NCEP–National Center for Atmospheric Research (NCAR) reanalysis (NNR) produce significant negative trends during 1979–2008 in September (also observed in the ERA-Interim reanalysis), which they attributed to particularly an intensification of the underlying cyclone central pressures in the Ross Sea region. However, Turner et al. (2013) note the negative MSLP trends in this region during spring may be sensitive to a remarkably deep ASL in September 2008. Examining the trends by month, Turner et al. (2013) note a significant ($p < 0.10$) deepening of the ASL in January, and also a deepening (but not significant) from April to May.

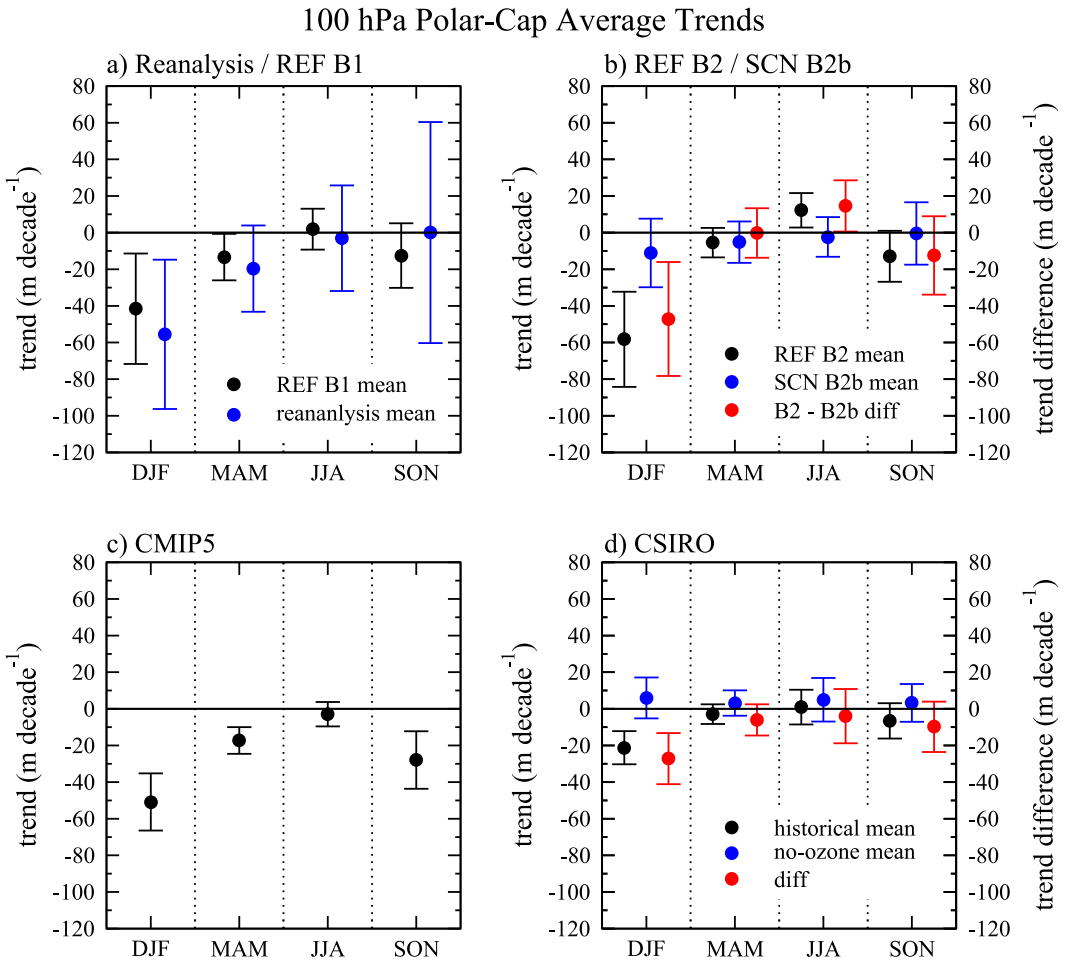

FIG. 4. Seasonal linear trends during 1979–2004 of 100-hPa geopotential height (in m decade^{-1}) over the polar cap (70°–90°S) for (a) REF-B1 mean and the reanalyses mean, (b) REF-B2 and SCN-B2b means, (c) CMIP5 means, and (d) CSIRO model ensemble means. Error bars represent the 95% confidence intervals for the multimodel mean/reanalysis trend. The red data display the trend differences between the REF-B2 and SCN-B2b trends in (b) and the CSIRO historical and no-ozone trends in (d).

In the model simulations, all ozone-containing simulations (REF-B2, CMIP5, and CSIRO historical simulation) have significant (at least $p < 0.10$) negative trends in DJF. However, the trend differences between REF-B2/SCN-B2b and the two groups of CSIRO simulations are not statistically significant in DJF, suggesting that while stratospheric ozone depletion is likely playing a role in deepening the ASL at 850 hPa (based on the CMIP5 ensemble mean in Fig. 6c), greenhouse gases are likely also contributing to the negative trends in REF-B2 (Fig. 6b) and the CSIRO historical simulations (Fig. 6d). The forcing from stratospheric ozone depletion is not distinguishable from other forcing agents in these simulations, consistent with some studies that demonstrate that austral summer trends in the SAM toward its positive polarity (which also deepens the ASL) may also be tied to a weaker forcing from greenhouse gases (Arblaster and Meehl 2006; Fogt et al. 2009a). Across the other seasons, the CMIP5 trends are also statistically significant in MAM; this will be discussed more later. The effect of the ozone hole in JJA as derived from the comparison between the REF-B2 and SCN-B2b runs is opposite to that derived from the comparison between the CSIRO historical and CSIRO no-ozone simulations (Figs. 4b and 4d). The reasons for this discrepancy are unclear and beyond the scope of the current study.

b. *Spatial height changes*

Based on the area-averaged approach, the primary impact of stratospheric ozone depletion is observed in the stratosphere and in austral summer; however, since this technique may mask important regional trends (or differences), spatial height trends/changes in the troposphere are now examined. To compare with Turner et al.

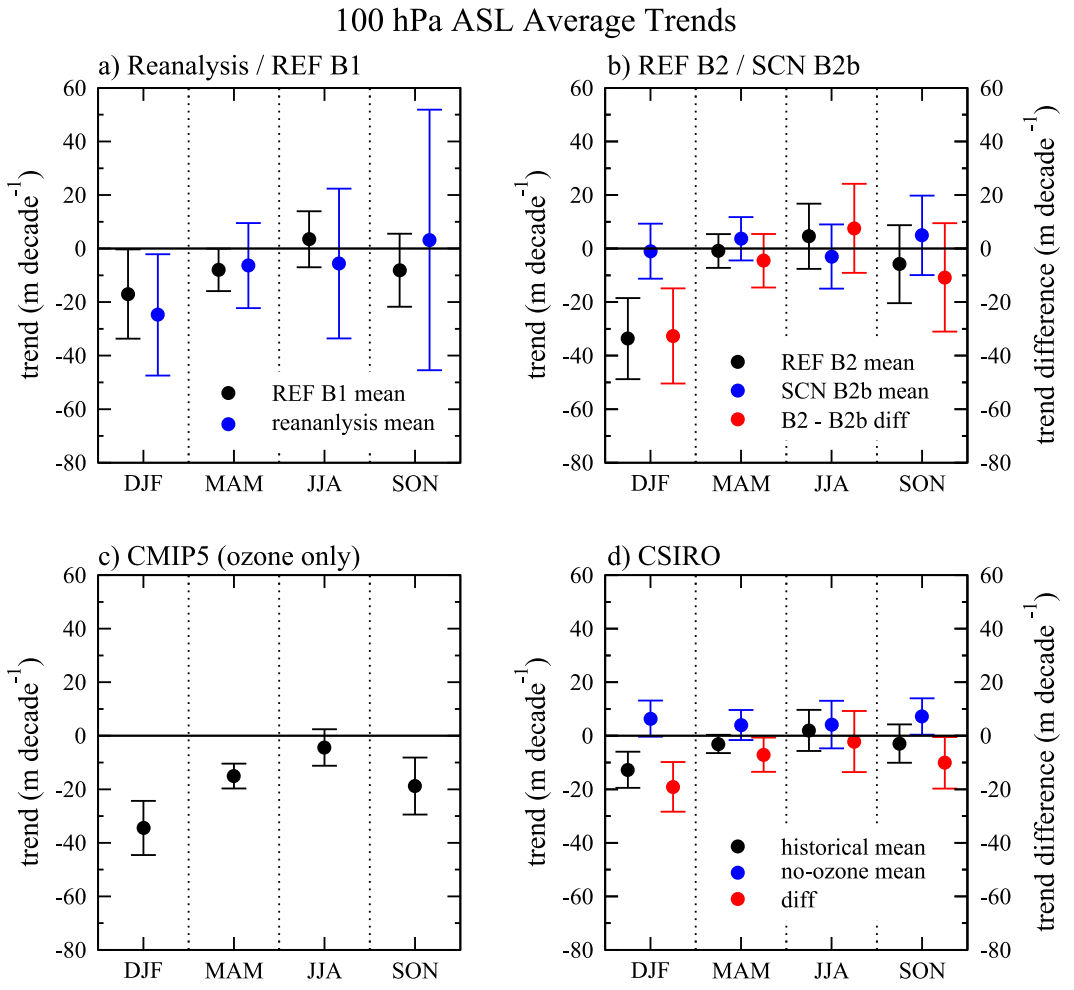

FIG. 5. As in Fig. 4, but for the averages in the ASL region.

(2009), seasonal height trends at 500 hPa are first examined in Fig. 7 (contours are multimodel mean trends over 1979–2004). In Fig. 7, the shading indicates either significant (as in Fig. 3, from dark to light, $p < 0.01$, $p < 0.05$, $p < 0.10$, respectively) differences between the REF-B2/SCN-B2b multimodel mean trends (first column), the CSIRO historical/CSIRO no-ozone model mean trends (second column), or simply in the CMIP5 multimodel mean trends. As such, the shading highlights the role of ozone forcing in the trends contoured in Fig. 7, which contain all historical forcings in the first two columns.

From the CCM simulations (left column in Fig. 7), significant ozone-related negative height trends (based on the shading as described previously) are observed in the ASL region off the coast of West Antarctica only in DJF; significant negative trends are also clearly present in the CMIP5 simulations (right column), but only weakly present (a small region in the Bellingshausen Sea of $p < 0.10$ trend difference) in the CSIRO model. The largest trends occurring in DJF is consistent with the multireanalysis mean in Figs. 3, 5, and 6, and with other recent work (Son et al. 2010; Polvani et al. 2011). Furthermore, the pattern of the height trends in DJF in all seasons, regardless of their statistical significance, projects strongly onto the positive phase of the SAM. Notably, there are no regions poleward of 60°S of positive height trends in the CMIP5 models (right column of Fig. 7), suggesting that the positive 500 hPa height trends in the REF-B2 simulations are due to the role of greenhouse gas changes, the positive ozone–SAM relationship in winter (Fogt et al. 2009b), and/or that they are partially offset by coupling to the ocean in the or tropospheric ozone increases in the CMIP5 simulations. Finally, the CMIP trends show significant height changes in the ASL region also in MAM, which may imply a secondary, smaller regional impact of stratospheric ozone depletion in MAM, perhaps related to coupling with an ocean as

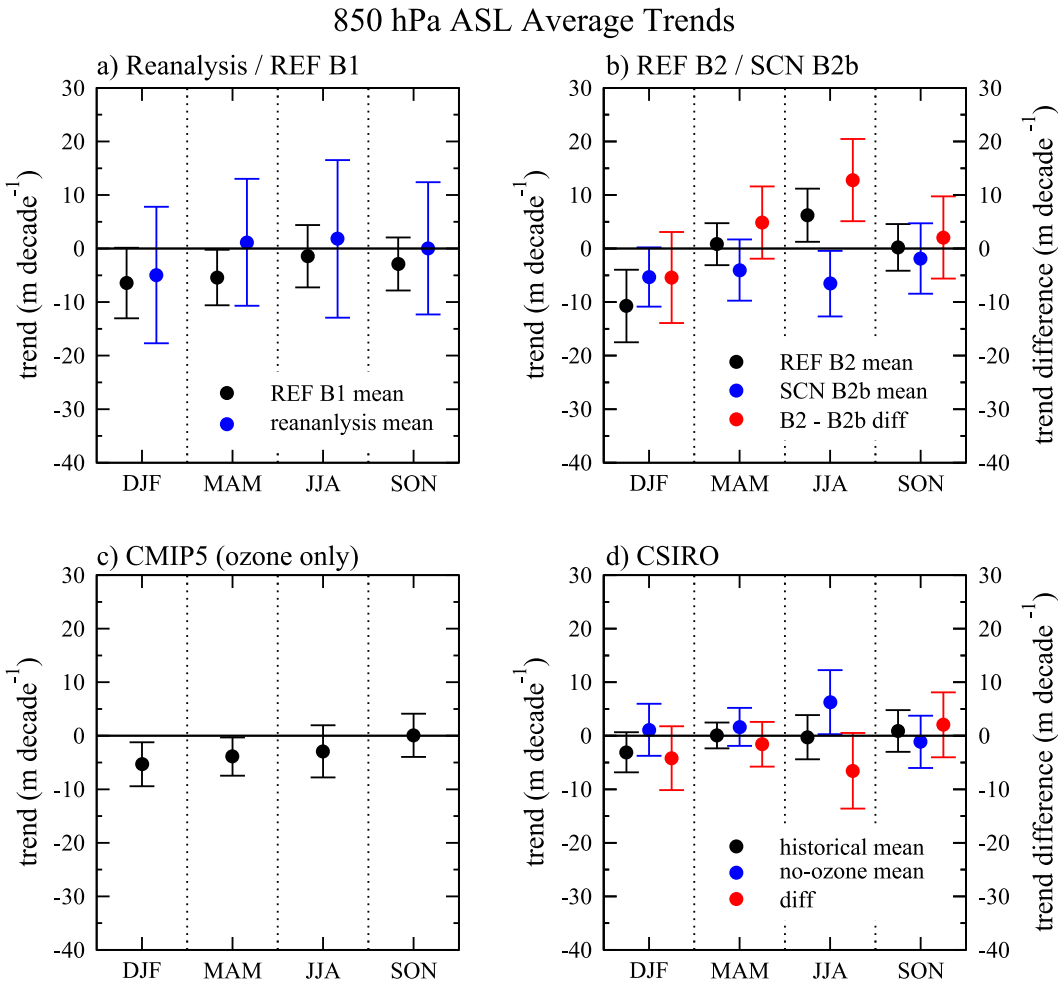

FIG. 6. As in Fig. 4, but for 850-hPa geopotential height in the ASL region.

negative trends (although not significantly different from the no-ozone simulations) are also seen in the CSIRO simulations (middle column of Fig. 7). Tropospheric ozone increases included in the CMIP5 simulations may also be contributing to these trends.

Figure 7 is primarily based on multimodel means, which helps in identifying the consistent forced response, but may mask important differences in individual models as observed in Turner et al. (2009). To more directly compare with Turner et al. (2009) and to better understand the sensitivity of the ozone response in MAM, height changes in individual models are examined in Fig. 8 (CCMs and CSIRO) and Fig. 9 (CMIP5 models). Similar to before, significance tests are based on the mean trend difference between simulations with all forcings and those without stratospheric ozone depletion (Fig. 8), or the multimodel mean trend (Fig. 9). From Fig. 8, the only REF-B2 simulation to show a statistically different negative trend from the SCN-B2b simulation in the ASL region is the CMAM model (Fig. 8b). Other simulations show significantly different positive REF-B2 trends (especially CCSRNIES and UMSLIMCAT), suggesting that the response in MAM in the CCMVal-2 on average is not only weaker (as reflected at 850 hPa in Fig. 6b), but also strongly model dependent. There is better agreement across the CMIP5 simulations (Fig. 9): all of the simulations show negative 500-hPa geopotential height trends in the ASL region during 1979–2004 in MAM, with two models indicating statistically significant trends in the ASL region (FGOALS, Fig. 9b; GISS_EH, Fig. 9c). The similarities across the CMIP5 models, as well as in the CMAM CCM, which is coupled to an ocean, point to a possible influence from stratospheric ozone depletion in this region that requires coupling to an ocean model in order to fully capture the negative height changes. However, the changes are still (on average) smaller than in DJF (Figs. 6 and 7) and to those discussed by Turner et al. (2009), who noted 500-hPa differences in the vicinity of the ASL around 50 m. Thus, any ozone influence on the regional circulation in the vicinity of the ASL in MAM is

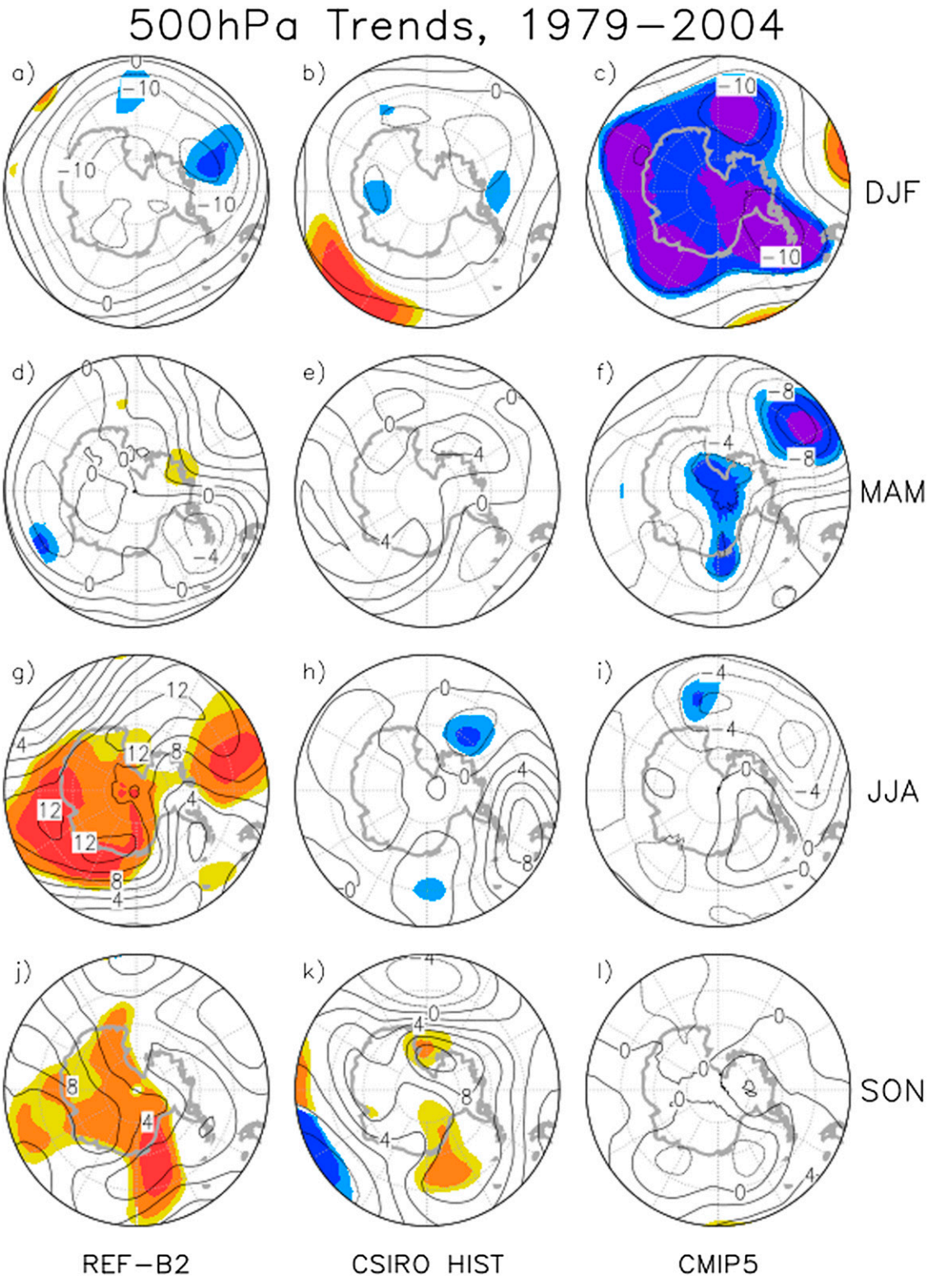

FIG. 7. 500-hPa geopotential height trends (1979–2004) for the (left) REF-B2 mean, (middle) CSIRO historical mean, and (right) CMIP5 multimodel mean. From left to right, shading (from darkest to lightest) indicates significant REF-B2 minus SCN-B2b trend differences, CSIRO historical minus CSIRO no-ozone trend differences, and multimodel mean CMIP5 trends at $p < 0.01$, $p < 0.05$, $p < 0.10$, respectively, for (a)–(c) DJF, (d)–(f) MAM, (g)–(i) JJA, and (j)–(l) SON. Contour interval is 5 m decade^{-1} in (a)–(c) and 2 m decade^{-1} elsewhere.

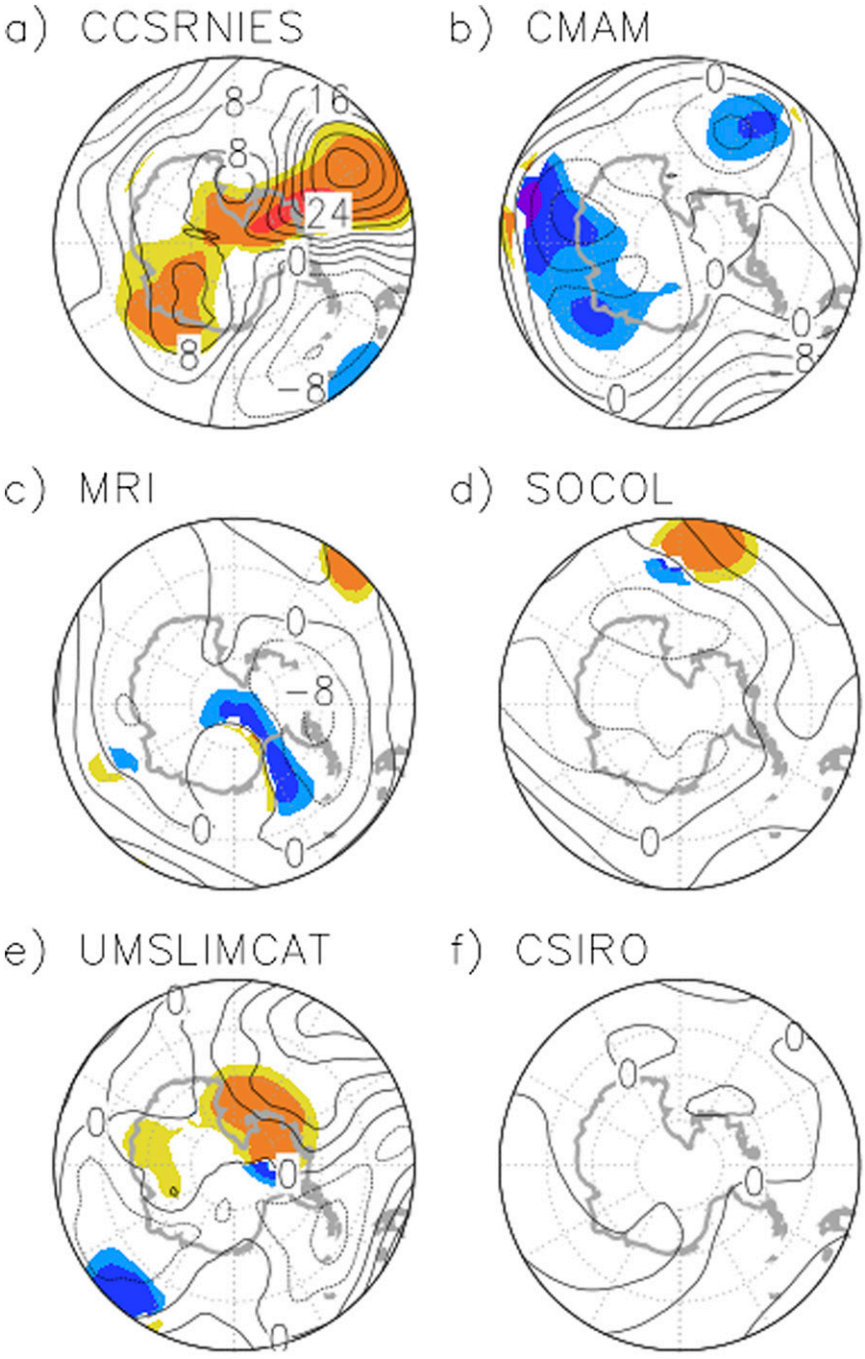

FIG. 8. MAM 500-hPa geopotential height trends (1979–2004) for (a)–(e) individual CCMVal-2 models and (f) the CSIRO historical simulation (as in Fig. 7e). Shading (from darkest to lightest) in (a)–(e) indicates significant REF-B2 minus SCN-B2b trend differences at $p < 0.01$, $p < 0.05$, and $p < 0.10$, respectively. Contour interval is 4 m decade^{-1}.

secondary to the changes in DJF, and model dependent. The impact of tropospheric ozone increases included in the CMIP5 simulations is not isolated here, but may contribute to some of the changes, and should be examined in further study.

Our analysis is concluded by examining the height trends at 850 hPa in Fig. 10, since the ASL is primarily a surface feature and ozone is known to also have influences on the surface climate (Thompson and Solomon 2002). With the exception of the austral summer (where

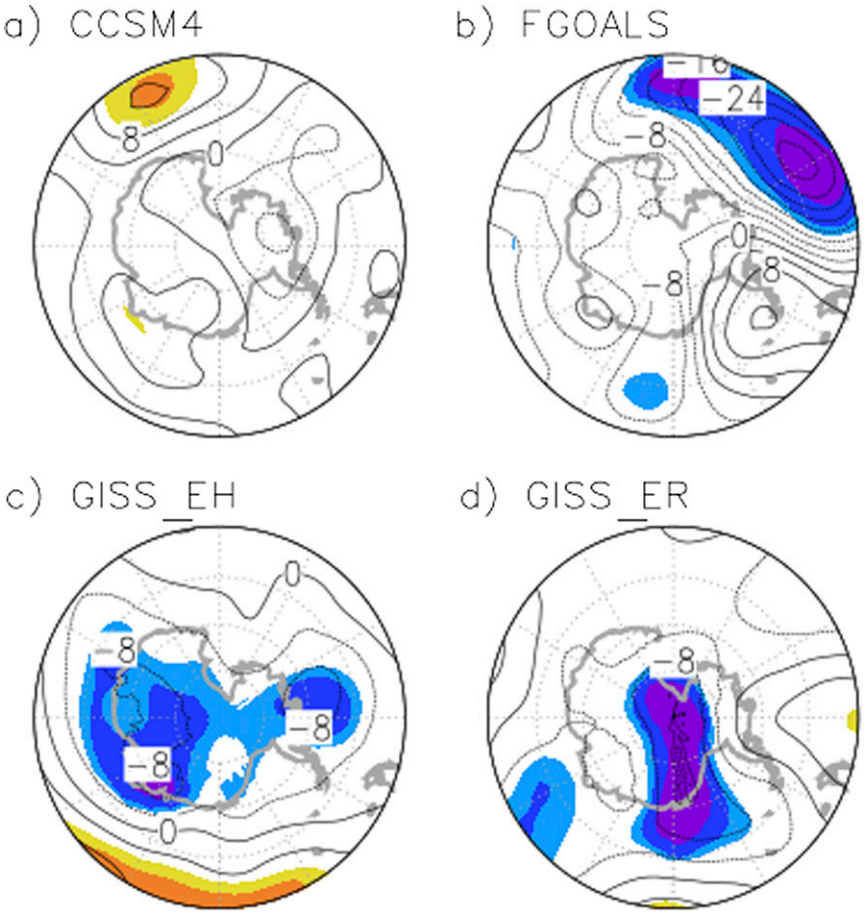

FIG. 9. MAM 500-hPa geopotential height trends (1979–2004) for individual CMIP5 ozone-only simulations. Shading (from darkest to lightest) indicates significant trends at $p < 0.01$, $p < 0.05$, and $p < 0.10$, respectively. Contour interval is 4 m decade^{-1}.

the model means indicate negative trends in the ASL, two of which are significantly related to stratospheric ozone depletion), the regions of statistical significance are smaller, and there is less agreement between the various model means. The reduction of significant regions is not too surprising in the lower troposphere given the large near-surface interannual variability in the high southern latitudes (Connolley 1997; Fogt et al. 2012; Turner et al. 2013), the different original model resolutions and therefore representation of Antarctica (which only lies below 850 hPa near the coasts; Tables 1 and 2), and the considerably weaker changes in the reanalysis in the lower troposphere (Figs. 3, 6). As before at 500 hPa, only the CMIP5 simulations demonstrate a significant relationship between ozone changes and the negative height trends at 850 hPa in the ASL region. The fact that only the CMIP5 simulations show a significant ozone response in MAM may be due to the importance of the coupling to the ocean model in influencing the lower troposphere; however, the trends in the CSIRO historical simulation in this season are much weaker (Fig. 10e), so it remains unclear how the different model configurations are influencing this result. Nonetheless, the spatial structure of the changes in austral summer in both the CCMs and CMIP5 models project strongly onto the positive polarity of the SAM, and are in agreement with previous analyses that showed a dominant influence of stratospheric ozone depletion on the near surface SAM changes in austral summer (Thompson and Solomon 2002; Arblaster and Meehl 2006; Miller et al. 2006; Perlwitz et al. 2008; Fogt et al. 2009a).

5. Discussion and conclusions

Using a suite of chemistry–climate models and historical simulations from the CMIP5 archive, the analysis presented herein has noted a profound impact from stratospheric ozone depletion on the atmospheric circulation over the Antarctic polar cap, most marked in the mid to upper stratosphere in austral spring (above 100 hPa) and troposphere in austral summer. These findings are consistent with

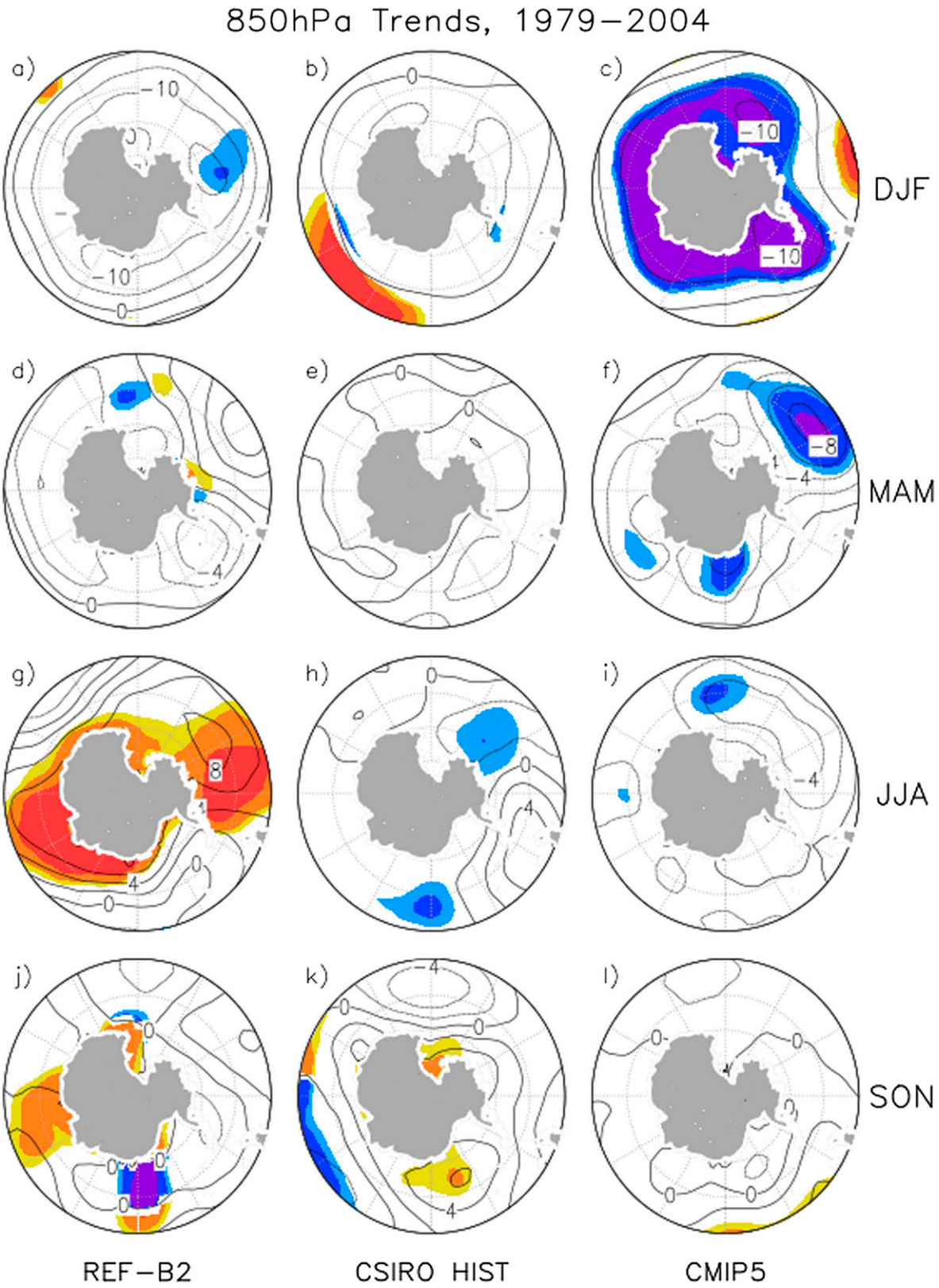

FIG. 10. As in Fig. 7, but for 850-hPa geopotential height.

a growing body of work noting a strengthening of the austral summer SAM index associated with historical stratospheric ozone depletion (e.g., Thompson and Solomon 2002; Miller et al. 2006; Arblaster and Meehl 2006; Perlwitz et al. 2008; Fogt et al. 2009a; Son et al. 2010). While the influence of stratospheric ozone depletion extends over the Amundsen and Bellingshausen Seas, the greatest atmospheric circulation changes in this region are observed in austral summer throughout the troposphere and stratosphere; a much weaker response, perhaps tied to stratospheric ozone depletion, is observed at 500 and 850 hPa in the CMIP5 simulations in austral autumn. Notably, the comparison between the CCMs and the CMIP5 models reveal that coupling to an ocean and other model differences may produce notable differences in the trends in the lower troposphere, with a more clear and consistent role of stratospheric ozone depletion outside of austral summer. Although broadly in agreement with Turner et al. (2009), who note a significant influence of stratospheric ozone depletion on the ASL in autumn, the results presented here demonstrate a much weaker response overall, barely above the large interannual variability characterizing the region. These findings build upon previous work, which has had a more hemispheric/large-scale, summer only, and/or zonally symmetric focus (e.g., Eyring et al. 2007; Perlwitz et al. 2008; Fogt et al. 2009b; Son et al. 2010; Sigmond et al. 2010; Polvani et al. 2011). However, the impact of tropospheric ozone increases (included in the CMIP5 simulations) on the atmospheric circulation changes has not been investigated explicitly in this study, and certainly warrants further study.

Austral autumn circulation changes in the Amundsen and Bellingshausen Seas have been shown to drive changes in the advance of sea ice (Stammerjohn et al. 2008) and its extent (Holland and Kwok 2012) as well as changes in the flux of circumpolar deep water and glacial melt (Steig et al. 2012). In many of these studies, it was remote changes in the tropical sea surface conditions that led to the changes in the circulation; here we suggest that atmospheric models which are coupled to an ocean display a possible secondary (weaker) ozone-forced change in the regional circulation, similar to that observed in austral summer. The ozone connections are much weaker in the winter and spring, consistent with the tropical influence on the warming in West Antarctica and the Antarctic Peninsula in austral winter and spring noted in previous studies (Schneider et al. 2012; Ding et al. 2011; Clem and Fogt 2013). Thus, it currently appears that outside of austral summer, the influence of stratospheric ozone depletion on the tropospheric circulation over and near Antarctica is much weaker, and remote forcing from the tropics often dominates. However, as ozone recovers and greenhouse gases continue to increase, more pronounced anthropogenic circulation changes, including their impacts on sea ice, glacial melt, and the regional climate, are likely to be observed across all seasons.

Acknowledgments. All authors acknowledge support from the National Science Foundation Office of Polar Programs Grant ANT-0944168. Thanks are extended to NCEP, ECMWF, and the Japanese Meteorological Agency for their reanalysis data. Additionally the authors thank the modeling groups for making their CCM simulations available for analysis, the Chemistry-Climate Model Validation (CCMVal) Activity for WCRP's (World Climate Research Programme) SPARC (Stratospheric Processes and their Role in Climate) project for coordinating the model data analysis activity, and the British Atmospheric Data Center for collecting and archiving the data. The CMIP5 data were obtained from the Earth System Grid Federation, and the various modeling centers are thanked for their historical simulations that contributed to this research study.

REFERENCES

Akiyoshi, H., and Coauthors, 2009: A CCM simulation of the breakup of the Antarctic polar vortex in the years 1980–2004 under the CCMVal scenarios. *J. Geophys. Res.,* **114,** D03103, doi:10.1029/2007JD009261.

Arblaster, J. M., and G. A. Meehl, 2006: Contributions of external forcings to southern annular mode trends. *J. Climate,* **19,** 2896–2905, doi:10.1175/JCLI3774.1.

Bodeker, G. E., J. C. Scott, K. Kreher, and R. L. McKenzie, 2001: Global trends in potential vorticity coordinates using TOMS and GOME intercompared against the Dobson network: 1978–1998. *J. Geophys. Res.,* **106,** 23 029–23 042, doi:10.1029/2001JD900220.

——, H. Shiona, and H. Eskes, 2005: Indicators of Antarctic ozone depletion. *Atmos. Chem. Phys.,* **5,** 2603–2615, doi:10.5194/acp-5-2603-2005.

Clem, K. R., and R. L. Fogt, 2013: Varying roles of ENSO and SAM on the Antarctic Peninsula climate in austral spring. *J. Geophys. Res. Atmos.,* **118,** 11 481–11 492, doi:10.1002/jgrd.50860.

Connolley, W. M., 1997: Variability in annual mean circulation in southern high latitudes. *Climate Dyn.,* **13,** 745–756, doi:10.1007/s003820050195.

Dee, D. P., and Coauthors, 2011: The ERA-Interim reanalysis: Configuration and performance of the data assimilation system. *Quart. J. Roy. Meteor. Soc.,* **137,** 553–597, doi:10.1002/qj.828.

Ding, Q., E. J. Steig, D. S. Battisti, and M. Küttel, 2011: Winter warming in West Antarctica caused by central tropical Pacific warming. *Nat. Geosci.,* **4,** 398–403, doi:10.1038/ngeo1129.

Eyring, V., and Coauthors, 2007: Multimodel projections of stratospheric ozone in the 21st century. *J. Geophys. Res.,* **112,** D16303, doi:10.1029/2006JD008332.

——, and Coauthors, 2008: Overview of the new CCMVal reference and sensitivity simulations in support of upcoming ozone and climate assessments and the planned SPARC CCMVal report. *SPARC Newsletter,* No. 30, SPARC Office, Toronto, ON, Canada, 20–26.

Fogt, R. L., J. Perlwitz, A. J. Monaghan, D. H. Bromwich, J. M. Jones, and G. J. Marshall, 2009a: Historical SAM variability. Part II: Twentieth-century variability and trends from reconstructions, observations, and the IPCC AR4 models. *J. Climate,* **22,** 5346–5365, doi:10.1175/2009JCLI2786.1.

——, ——, S. Pawson, and M. A. Olsen, 2009b: Intra-annual relationships between polar ozone and the SAM. *Geophys. Res. Lett.,* **36,** L04707, doi:10.1029/2008GL036627.

——, A. J. Wovrosh, R. A. Langen, and I. Simmonds, 2012: The characteristic variability and connection to the underlying synoptic activity of the Amundsen – Bellingshausen Seas Low. *J. Geophys. Res.,* **117,** D07111, doi:10.1029/2011JD017337.

Gillett, N. P., J. C. Fyfe, and D. E. Parker, 2013: Attribution of observed sea level pressure trends to greenhouse gases, aerosol, and ozone change. *Geophys. Res. Lett.,* **40,** 2302–2306, doi:10.1002/grl.50500.

Hio, Y., and S. Yoden, 2005: Interannual variations of the seasonal march in the Southern Hemisphere stratosphere for 1979–2002 and characterization of the unprecedented year in 2002. *J. Atmos. Sci.,* **62,** 567–580, doi:10.1175/JAS-3333.1.

Holland, P. R., and R. Kwok, 2012: Wind-driven trends in Antarctic sea-ice drift. *Nat. Geosci.,* **5,** 872–875, doi:10.1038/ngeo1627.

Hosking, J. S., A. Orr, G. J. Marshall, J. Turner, and T. Phillips, 2013: The influence of the Amundsen-Bellingshausen Seas low on the climate of West Antarctica and its representation in coupled climate model simulations. *J. Climate,* **26,** 6633–6648, doi:10.1175/JCLI-D-12-00813.1.

Kindem, I. T., and B. Christiansen, 2001: Tropospheric response to stratospheric ozone loss. *Geophys. Res. Lett.,* **28,** 1547–1551, doi:10.1029/2000GL012552.

Lachlan-Cope, T. A., W. M. Connolley, and J. Turner, 2001: The role of the non-axisymmetric Antarctic orography in forcing the observed pattern of variability of the Antarctic climate. *Geophys. Res. Lett.,* **28,** 4111–4114, doi:10.1029/2001GL013465.

Marshall, G. J., 2003: Trends in the southern annular mode from observations and reanalyses. *J. Climate,* **16,** 4134–4143, doi:10.1175/1520-0442(2003)016<4134:TITSAM>2.0.CO;2.

——, 2007: Half-century seasonal relationships between the southern annular mode and Antarctic temperatures. *Int. J. Climatol.,* **27,** 373–383, doi:10.1002/joc.1407.

——, A. Orr, N. P. M. van Lipzig, and J. C. King, 2006: The impact of a changing Southern Hemisphere annular mode on Antarctic Peninsula summer temperatures. *J. Climate,* **19,** 5388–5404, doi:10.1175/JCLI3844.1.

Massom, R., S. Stammerjohn, W. Lefebvre, S. Harangozo, N. Adams, T. Scambos, M. Pook, and C. Fowler, 2008: West Antarctic Peninsula sea ice in 2005: Extreme ice compaction and ice edge retreat due to strong anomaly with respect to climate. *J. Geophys. Res.,* **113,** C02S20, doi:10.1029/2007JC004239.

Miller, R. L., G. A. Schmidt, and D. T. Shindell, 2006: Forced annular variations in the 20th century Intergovernmental Panel on Climate Change Fourth Assessment Report models. *J. Geophys. Res.,* **111,** D18101, doi:10.1029/2005JD006323.

Morgenstern, O., and Coauthors, 2010: Review of the formulation of present-generation stratospheric chemistry–climate models and associated external forcings. *J. Geophys. Res.,* **115,** D00M02, doi:10.1029/2009JD013728.

O'Donnell, R., N. Lewis, S. McIntyre, and J. Condon, 2011: Improved methods for PCA-based reconstructions: Case study using the Steig et al. (2009) Antarctic temperature reconstruction. *J. Climate,* **24,** 2099–2115, doi:10.1175/2010JCLI3656.1.

Onogi, K., and Coauthors, 2005: JRA-25: Japanese 25-Year Re-Analysis Project: Progress and status. *Quart. J. Roy. Meteor. Soc.,* **131,** 3259–3268, doi:10.1256/qj.05.88.

Orr, A., G. J. Marshall, J. C. R. Hunt, J. Sommeria, C.-G. Wang, N. P. M. van Lipzig, D. Cresswall, and J. C. King, 2008: Characteristics of summer airflow over the Antarctic Peninsula in response to recent strengthening of the westerly circumpolar winds. *J. Atmos. Sci.,* **65,** 1396–1413, doi:10.1175/2007JAS2498.1.

Perlwitz, J., S. Pawson, R. L. Fogt, J. E. Nielsen, and W. D. Neff, 2008: Impact of stratospheric ozone hole recovery on Antarctic climate. *Geophys. Res. Lett.,* **35,** L08714, doi:10.1029/2008GL033317.

Polvani, L. M., D. W. Waugh, G. J. P. Correa, and S.-W. Son, 2011: Stratospheric ozone depletion: The main driver of twentieth-century atmospheric circulation changes in the Southern Hemisphere. *J. Climate,* **24,** 795–811, doi:10.1175/2010JCLI3772.1.

Randel, W., and F. Wu, 1999: Cooling of the Arctic and Antarctic polar stratospheres due to ozone depletion. *J. Climate,* **12,** 1467–1479, doi:10.1175/1520-0442(1999)012<1467:COTAAA>2.0.CO;2.

Raphael, M. N., 2004: A zonal wave 3 index for the Southern Hemisphere. *Geophys. Res. Lett.,* **31,** L23212, doi:10.1029/2004GL020365.

Roscoe, H. K., J. D. Shanklin, and S. R. Colwell, 2005: Has the Antarctic vortex split before 2002? *J. Atmos. Sci.,* **62,** 581–588, doi:10.1175/JAS-3331.1.

Saha, S., and Coauthors, 2010: The NCEP Climate Forecast System Reanalysis. *Bull. Amer. Meteor. Soc.,* **91,** 1015–1057, doi:10.1175/2010BAMS3001.1.

Schneider, D. P., C. Deser, and Y. Okumura, 2012: An assessment and interpretation of the observed warming of West Antarctica in the austral spring. *Climate Dyn.,* **38,** 323–347, doi:10.1007/s00382-010-0985-x.

Sigmond, M., and J. C. Fyfe, 2014: The Antarctic sea ice response to the ozone hole in climate models. *J. Climate,* **27,** 1336–1342, doi:10.1175/JCLI-D-13-00590.1.

——, ——, and J. F. Scinocca, 2010: Does the ocean impact the atmospheric response to stratospheric ozone depletion? *Geophys. Res. Lett.,* **37,** L12706, doi:10.1029/2010GL043773.

Son, S.-W., and Coauthors, 2010: Impact of stratospheric ozone on Southern Hemisphere circulation change: A multimodel assessment. *J. Geophys. Res.,* **115,** D00M07, doi:10.1029/2010JD014271.

SPARC CCMVal, 2010: SPARC report on the evaluation of chemistry–climate models. V. Eyring, T. G. Shepherd, and D. W. Waugh, Eds., SPARC Rep. 5, 426 pp. [Available online at http://www.sparc-climate.org/publications/sparc-reports/sparc-report-no5/.]

Stammerjohn, S. E., D. G. Martinson, R. C. Smith, X. Yuan, and D. Rind, 2008: Trends in Antarctic annual sea ice retreat and advance and their relation to El Niño–Southern Oscillation and southern annular mode variability. *J. Geophys. Res.,* **113,** C03S90, doi:10.1029/2007JC004269.

Steig, E. J., D. P. Schneider, S. D. Rutherford, M. E. Mann, J. C. Comiso, and D. T. Shindell, 2009: Warming of the Antarctic ice-sheet surface since the 1957 International Geophysical Year. *Nature,* **457,** 459–462, doi:10.1038/nature07669.

——, Q. Ding, D. S. Battisti, and A. Jenkins, 2012: Tropical forcing of circumpolar deep water inflow and outlet glacier thinning in the Amundsen Sea Embayment, West Antarctica. *Ann. Glaciol.,* **53,** 19–28, doi:10.3189/2012AoG60A110.

Taylor, K. E., R. J. Stouffer, and G. A. Meehl, 2012: An overview of CMIP5 and the experiment design. *Bull. Amer. Meteor. Soc.,* **93,** 485–498, doi:10.1175/BAMS-D-11-00094.1.

Thompson, D. W., and S. Solomon, 2002: Interpretation of recent Southern Hemisphere climate change. *Science,* **296,** 895–899, doi:10.1126/science.1069270.

Turner, J., and Coauthors, 2009: Non-annular atmospheric circulation change induced by stratospheric ozone depletion and its role in the recent increase of Antarctic sea ice extent. *Geophys. Res. Lett.,* **36,** L08502, doi:10.1029/2009GL037524.

——, T. Phillips, J. S. Hosking, G. J. Marshall, and A. Orr, 2013: The Amundsen Sea low. *Int. J. Climatol.,* **33,** 1818–1829, doi:10.1002/joc.3558.

WMO, 2011: Scientific assessment of ozone depletion: 2010. Global Ozone Research and Monitoring Project Rep. 52, World Meteorological Organization/United Nations Environmental Programme, 516 pp. [Available online at http://www.esrl.noaa.gov/csd/assessments/ozone/2010/report.html.]

Zwally, H. J., J. C. Comiso, C. L. Parkinson, D. J. Cavalieri, and P. Gloersen, 2002: Variability of Antarctic sea ice 1979–1998. *J. Geophys. Res.,* **107,** 3041, doi:10.1029/2000JC000733.